



An internal model control design method for failure-tolerant control with multiple objectives[☆]

Ali Mesbah^{a,*}, Joel A. Paulson^b, Richard D. Braatz^c

^a Department of Chemical and Biomolecular Engineering, University of California-Berkeley, Berkeley, CA 94720, USA

^b Department of Chemical and Biomolecular Engineering, The Ohio State University, Columbus, OH 43210, USA

^c Department of Chemical Engineering, Massachusetts Institute of Technology, Cambridge, MA 02139, USA

ARTICLE INFO

Article history:

Received 29 January 2020

Revised 27 April 2020

Accepted 1 June 2020

Available online 6 June 2020

Keywords:

Control systems with multiple objectives

Failure-tolerant control

Internal model control

ABSTRACT

The selection of control structure is a critical step in the design of a control system since it can largely affect the achievable control performance. This paper presents a general internal model control (IMC) structure with multiple degrees-of-freedom for the design of control systems with multiple objectives (i.e., reference tracking and load and output disturbance rejection), so that controllers are designed independently of each other. The optimal performance of controllers is shown to remain intact when a controller is taken off-line, for example, due to actuator and/or sensor failures. This feature circumvents the need to redesign the remaining on-line controllers for optimal failure-tolerant control. The proposed control approach is used to derive IMC control structures for multi-loop cascade and coordinated control systems. The performance of the control approach is demonstrated on a simulated thin-film drying process in continuous pharmaceutical manufacturing for several multi-loop control structures and a variety of control-loop component failures.

© 2020 Elsevier Ltd. All rights reserved.

1. Introduction

The design of the control structure, which is the specification of the interconnection of measurements, exogenous inputs, and manipulated variables, greatly influences the performance achievable by a control system. In practice, control systems are commonly required to fulfill multiple objectives in terms of reference tracking and load and output disturbance rejection, which cannot be adequately specified using a single performance measure. This realization has led to the development of numerous control structures that have multiple degrees-of-freedom, where each degree-of-freedom is tasked with addressing some subset of the control objectives (Grimble, 1988; Brosilow and Markale, 1992; Limebeer et al., 1993; Pottmann et al., 1996; Zhou and Ren, 2001; Dehghani et al., 2006; Vilanova et al., 2006; Liu et al., 2007; Vidyasagar, 2011). As failures in system components inevitably occur in practice, an important practical consideration in control structure selection is to ensure that the selected control structure and its associated controllers have graceful performance degradation during

component failures (Blanke et al., 2003; Isermann, 2006; Zhou and Frank, 1998; paulson 2019).

Internal model control (IMC) (Morari and Zafriou, 1989) is a control design method developed in the 1970s–1980s with several useful features, including that it provides a convenient theoretical framework for the design of two degrees-of-freedom control systems (i.e., feedback and feedforward controller) when model uncertainty is present (Vilanova, 2007). The basic idea of IMC control design is to combine an optimal controller obtained from the nominal process model with a low-pass filter to tradeoff closed-loop performance with robustness to model uncertainties. As the IMC structure is a particular case of the Youla-Jabr-Bongiorno-Kucera (or Youla for short) parametrization of controllers that preserve closed-loop stability, the original control design problem can be replaced by simply the selection of an arbitrary parameter that appears affinely in the closed-loop transfer function. This allows the IMC control structure to ensure internal nominal stability of the closed-loop system (Morari and Zafriou, 1989; Braatz, 1996). Furthermore, the IMC control structure allows for separate controller design for performance and robustness to alleviate the tradeoff between performance and robustness in the traditional feedback framework (Zhou and Ren, 2001).

This paper addresses the IMC control design with optimal failure tolerance. An extension of the IMC control structure is presented for failure-tolerant control with multiple objectives related

[☆] This work is an extension of the paper presented at the 2013 European Control Conference (Mesbah and Braatz, 2013).

* Corresponding author.

E-mail address: mesbah@berkeley.edu (A. Mesbah).

to reference tracking and rejection of load and output disturbances. The proposed IMC control structure enables the design of control systems with multiple degrees-of-freedom, where a controller for each exogenous input is designed independently of the other controllers. Thus, the control structure preserves the optimal performance of the remaining controllers when any of the controllers are taken off-line (e.g., due to actuator and/or sensor failures). That is, without compromising the best achievable control performance, the proposed IMC control structure alleviates the inherent suboptimality of a classical feedback control structure in dealing with failures of one or more controllers in a control system with multiple objectives. Additionally, the proposed IMC approach to failure tolerance is distinct from robust control methods that account for potential actuator and/or sensor failures in that these methods can result in overly conservative performance when no actuator and/or sensor failures occur. This is because the control system is designed with respect to worst-case performance in robust control methods (e.g., see Zhou and Ren, 2001).

The proposed multiple degrees-of-freedom IMC controller design approach is also extended for the design of multi-loop control systems by deriving a general control structure for multi-loop cascade and coordinated control systems. The performance of the control approach is demonstrated using a thin-film drying process in continuous pharmaceutical manufacturing (Mesbah et al., 2014).

Notation and Preliminaries. Throughout the paper, a finite-dimensional process is denoted by $P(s) \in \mathcal{RH}_\infty$, where s is the Laplace variable and \mathcal{RH}_∞ denotes the real rational subspace of \mathcal{H}_∞ consisting of all proper and rational transfer matrices. The exogenous inputs are bounded signals, i.e., $r, l_m, l_u, d_m, d_u \in \mathcal{L}_p[0, \infty)$, where $\mathcal{L}_p[0, \infty)$ encompasses all signal sequences on $[0, \infty)$ that have finite p -norm. The real-valued function $\|\cdot\|$ denotes any norm defined over the linear vector space of the signals. The induced system norm $|\cdot|$ is defined as the supremum of an output signal norm over a norm-bounded set of an input signal (Zhou et al., 1996).

Definition 1. (Internal Stability (Morari and Zafriou, 1989)): A linear time-invariant (LTI) closed-loop system is *internally stable* if transfer functions between all bounded exogenous inputs to the closed-loop system and all outputs are stable (i.e., have all poles in the open left-half plane).

Definition 2. (Robust Stability (Morari and Zafriou, 1989)): A closed-loop system is *robustly stable* if the controller C ensures the internal stability of the closed-loop system for all $P \in \mathcal{P}$, where \mathcal{P} is the set of uncertain processes.

2. Controller design with multiple objectives

A fundamental consideration in design of a control system is the choice of the control structure, which should not limit the achievable control performance. A general control structure for a process P with manipulated variable u , reference r , measured load disturbance l_m , unmeasured load disturbance l_u , measured output disturbance d_m , unmeasured output disturbance d_u , and measurement noise n is shown in Fig. 1.¹ All measured variables are fed directly into the controllers $C = [C_r C_{d_m} C_{l_m} C_y]$ that are tasked to ensure (i) the internal stability of the closed-loop system, (ii) the output y closely tracks the reference r (i.e., small error $e = y - r$), and (iii) the effects of measurement noise and measured and unmeasured disturbances on the closed-loop error e are suppressed. The mapping between the exogenous inputs to the closed-loop system

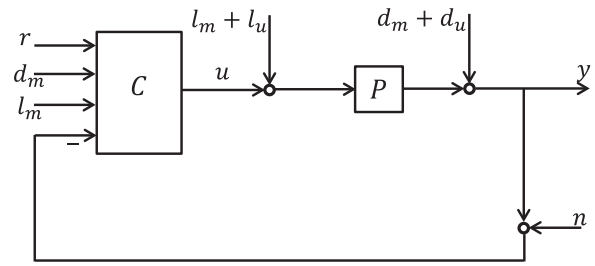


Fig. 1. A general classical feedback control structure, where $C = [C_r C_{d_m} C_{l_m} C_y]$ such that $u = C_r r + C_{d_m} d_m + C_{l_m} l_m + C_y y$.

and the process output and manipulated variable is described by

$$\begin{bmatrix} y \\ u \end{bmatrix} = \mathbf{H}(P, C) \begin{bmatrix} r \\ l_m \\ l_u \\ d_m \\ d_u \\ n \end{bmatrix}, \quad (1)$$

where the transfer function matrix $\mathbf{H}(P, C)$ is

$$\mathbf{H}(P, C) = \begin{bmatrix} H_{y,r} & H_{y,l_m} & H_{y,l_u} & H_{y,d_m} & H_{y,d_u} & H_{y,n} \\ H_{u,r} & H_{u,l_m} & H_{u,l_u} & H_{u,d_m} & H_{u,d_u} & H_{u,n} \end{bmatrix}, \quad (2)$$

with elements given explicitly in terms of P and C by

$$\begin{aligned} H_{y,r} &= \frac{PC_r}{1 + PC_y}, & H_{u,r} &= \frac{C_r}{1 + PC_y}, \\ H_{y,l_m} &= \frac{PC_{l_m}}{1 + PC_y} + \frac{P}{1 + PC_y}, & H_{u,l_m} &= \frac{C_{l_m}}{1 + PC_y} - \frac{C_y P}{1 + PC_y}, \\ H_{y,l_u} &= \frac{P}{1 + PC_y}, & H_{u,l_u} &= \frac{-C_y P}{1 + PC_y}, \\ H_{y,d_m} &= \frac{PC_{d_m}}{1 + PC_y} + \frac{1}{1 + PC_y}, & H_{u,d_m} &= \frac{C_{d_m}}{1 + PC_y} - \frac{C_y}{1 + PC_y}, \\ H_{y,d_u} &= \frac{1}{1 + PC_y}, & H_{u,d_u} &= \frac{-C_y}{1 + PC_y}, \\ H_{y,n} &= \frac{-PC_y}{1 + PC_y}, & H_{u,n} &= \frac{-C_y}{1 + PC_y}. \end{aligned}$$

Note that we have dropped the dependence of the plant and controllers on the Laplace variable s . This convention will be used throughout the rest of the paper for notational simplicity, unless otherwise needed for clarity.

Optimal control approaches commonly involve formulating a single performance measure in terms of an overall norm (such as a weighted H_2 - or H_∞ -norm) of the transfer matrix $\mathbf{H}(P, C)$ (Zhou et al., 1996). However, a drawback of these approaches is that defining a single closed-loop performance measure may not directly reflect multiple control objectives (e.g., reference tracking and disturbance rejection). A typical control problem has multiple objectives that are independently defined in terms of the relationships between specific exogenous inputs and specific outputs. Several of the closed-loop transfer functions in (2) that relate the exogenous inputs to the output y and manipulated variable u are functions of multiple controller transfer functions. Hence, the controller transfer functions cannot be designed independently to satisfy multiple independently defined control objectives. Here, we present an alternative control structure that is provably general while having each term in the relationship between an input exogenous and output as a function of only one controller transfer function.

Consider the internal model control structure in Fig. 2, where $Q = [Q_r Q_{d_m} Q_{l_m} Q_y]$ are IMC controllers. For the class of linear time-

¹ To simplify the exposition, explicit transfer functions for the various disturbances are not shown. Generalization of the results of this paper to include the disturbance transfer functions is straightforward.

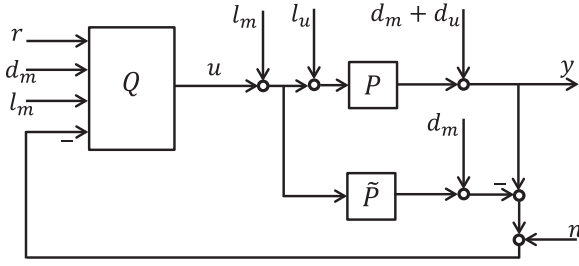


Fig. 2. The proposed general internal model control structure for a LTI system, where $Q = [Q_r, Q_{d_m}, Q_{l_m}, Q_y]$ are IMC controllers.

invariant systems, Theorem 1 states that the control structure depicted in Fig. 2 provides a non-restrictive framework for controller design with multiple objectives in terms of reference tracking and rejection of load and output disturbances.

Theorem 1. Suppose P is a transfer function of a stable LTI plant with measured output y , manipulated input u , measurement noise n , and disturbances $l_m, l_u, d_m,$ and d_u . Further, let Ω denote the set of stable functions of s . Then, the IMC control structure in Fig. 2, under the assumption of a perfect model $P = \tilde{P}$, has a one-to-one relationship with the classical feedback control structure in Fig. 1. As such, there is an invertible transformation between controllers $C = [C_r, C_{d_m}, C_{l_m}, C_y]$ and $Q = [Q_r, Q_{d_m}, Q_{l_m}, Q_y]$ that preserves the closed-loop transfer function matrix

$$C_y = \frac{Q_y}{1 - PQ_y}, \quad C_r = \frac{Q_r}{1 - PQ_y}, \quad C_{l_m} = \frac{Q_{l_m}}{1 - PQ_y}, \quad C_{d_m} = \frac{Q_{d_m}}{1 - PQ_y}, \quad (3)$$

$$Q_y = \frac{C_y}{1 + PC_y}, \quad Q_r = \frac{C_r}{1 + PC_y}, \quad Q_{l_m} = \frac{C_{l_m}}{1 + PC_y}, \quad Q_{d_m} = \frac{C_{d_m}}{1 + PC_y}. \quad (4)$$

In addition, the IMC control structure in Fig. 2 is internally stable if and only if each IMC controller Q_i is stable. This implies that the set of controllers $\{C$ given by (3) $\forall Q_y, Q_r, Q_{l_m}, Q_{d_m} \in \Omega\}$ contains all controllers C that stabilize P .

Proof. The first part of the proof follows by comparing $H(P, C)$ in (2) to the transfer function matrix for the IMC control structure as given by

$$H(P, Q) = \begin{bmatrix} PQ_r & P(1 + Q_{l_m}) & (1 - PQ_y)P & 1 + PQ_{d_m} & 1 - PQ_y & -PQ_y \\ Q_r & Q_{l_m} & -Q_y P & Q_{d_m} & -Q_y & -Q_y \end{bmatrix}. \quad (5)$$

By substituting (3) into this expression and applying simple algebraic manipulations, we can see that $H(P, Q) = H(P, C)$ holds. Since the function (3) has a well-defined inverse (4), given a Q we can always derive a unique C and vice versa. The first claim of the theorem directly follows. Note that this result is closely related to the well-known Youla parametrization, which is an important and fundamental result in control theory.

The second part of the proof follows from inspection of (5). The IMC control structure is internally stable if and only if all elements of $H(P, Q)$ are stable. When P is stable, these transfer functions are stable if and only if $Q_y, Q_r, Q_{l_m},$ and Q_{d_m} are stable (see Remark 1 for when P is unstable). Due to the established relationship between C and Q , two properties hold: (i) given any stable Q , the corresponding C given by (3) results in $H(P, C)$ being internally stable, and (ii) given any internally stabilizing C , the corresponding Q given by (4) must be stable. In other words, the elements of Q being stable is a necessary and sufficient condition for C producing a stable feedback structure, which leads to and the last claim of the theorem. \square

Remark 1. In Theorem 1, the plant P can be multi-input multi-output. Furthermore, when P is unstable, the internal stability of

the closed-loop system will be satisfied if PQ_y and $(1 - PQ_y)P$ are stable (Morari and Zafiriou, 1989; Tan et al., 2003).

The control structure in Fig. 2 is an extension of the IMC structure to systems with four degrees of freedom. Theorem 1 indicates that the proposed IMC control structure does not restrict the set of closed-loop transfer functions that ensure internal stability of the closed-loop system. Hence, this result implies that the use of the proposed IMC control structure does not limit the achievable closed-loop performance, regardless of the closed-loop performance measure(s) used to encode the control objectives. These characteristics are in contrast to most control structures that have been proposed for designing control systems with multiple degrees-of-freedom (e.g., see Skogestad and Postlethwaite, 1996 and the references therein).

Furthermore, the proposed IMC control structure provides a convenient framework for controller design with multiple objectives. This is because the closed-loop transfer matrix (5) depends on Q in an affine manner, and all columns depend on only one element of Q . Thus, the optimal controllers $Q_r, Q_{l_m}, Q_{d_m},$ and Q_y can be designed independently to realize multiple control objectives irrespective of the design of the other IMC controllers. The only tradeoff in designing the controllers $Q_r, Q_{l_m},$ and Q_{d_m} is that a fast speed of response (the effect on y) will be associated with faster and larger changes in the manipulated variable u . In addition, the design of Q_y requires prioritizing the multiple control objectives in view of their importance, as Q_y is the only controller that can suppress the effects of unmeasured disturbances and measurement noise. Next, we show how the control structure in Fig. 2 enables realizing the optimal achievable control performance in the presence of system failures.

Remark 2. Although the results presented above consider finite-dimensional, continuous-time LTI systems (that is, all transfer functions belong to \mathcal{RH}_∞), the proposed IMC control structure can also be applied to infinite-dimensional systems and to discrete-time systems; the former by defining the appropriate infinite-dimensional algebra (Curtain and Zwart, 1995; Mesbah et al., 2013) and the latter by replacing the Laplace transform with z-transform and the location of the poles for specifying stability of a transfer function.

3. Failure-tolerant control with multiple control objectives

A common approach to failure-tolerant control involves designing a single control system using robust control methods to deal with all potential actuator and/or sensor failures (e.g., see Zhou and Ren, 2001). Since in this approach the control system is designed with respect to worst-case performance, it may lead to overly conservative performance when no actuator and/or sensor failures occur. A distinct feature of the proposed IMC control structure is that the controllers $Q_r, Q_{l_m}, Q_{d_m},$ and Q_y can be designed independently from each other since only one controller appears in each column of (5). Therefore, the controllers do not have to be redesigned when a system component (e.g., actuator or sensor) is taken out of service due to a failure. In other words, each individual controller will remain optimal with respect to its objective when any of the other controllers is taken out of service (i.e., set to 0). This is an important advantage of the proposed IMC control structure in Fig. 2 when compared to the classical control structure in Fig. 1 that requires all the controllers to be designed simultaneously, as robustness or stability properties of controllers can be lost when a failure occurs unless all controllers are redesigned.

The proposed control structure also enables robust fault-tolerant control when abnormal system operation results from changes in process dynamics and/or disturbance characteristics. When changes in process dynamics can be characterized by model

uncertainty, the lower P in Fig. 2 is replaced with a process model $\tilde{P} \in \mathcal{P}$. In this case, the internal stability of the closed-loop system in Fig. 2 for any $\tilde{P} \in \mathcal{P}$ depends on Q_y only.

Theorem 2. For stable Q_r , Q_{l_m} , and Q_{d_m} , robust stability of the closed-loop system in Fig. 2 only depends on Q_y , \tilde{P} , and \mathcal{P} , where \mathcal{P} is the set of uncertain processes.

Proof. Consider that the process dynamics are described by the model \tilde{P} that belongs to the uncertainty set \mathcal{P} . Replace the lower P in Fig. 2 with \tilde{P} . The closed-loop transfer matrix $\mathbf{H}(P, Q)$ for the mapping between $[y, u]^T$ and the exogenous inputs (see (1)) takes the form

$$\begin{bmatrix} PQ_r S & PQ_{l_m} S + (I - \tilde{P}Q_y)SP & (I - \tilde{P}Q_y)SP & PQ_{d_m} S + (I - \tilde{P}Q_y)S & (I - \tilde{P}Q_y)S & -PQ_y S \\ Q_r S & Q_{l_m} S - Q_y SP & -Q_y SP & Q_{d_m} S - Q_y S & -Q_y S & -Q_y S \end{bmatrix}, \quad (6)$$

where S is

$$S = (I + (P - \tilde{P})Q_y)^{-1}.$$

Robust stability of the proposed control structure in Fig. 2 requires that all transfer functions in (6) be stable for any $\tilde{P} \in \mathcal{P}$. For stable controllers Q_r , Q_{l_m} , and Q_{d_m} , (6) indicates that the robust stability of the closed-loop system is determined by the stability of S . Hence, the robust stability of the system in Fig. 2 only hinges on Q_y , \tilde{P} , and \mathcal{P} . \square

Theorem 2 implies that as long as controllers Q_r , Q_{l_m} , and Q_{d_m} are stable, they will not influence the internal stability of the closed-loop system in the presence of model uncertainties. This observation motivates a robust fault-tolerant control approach similar to that in (Zhou and Ren, 2001), where Q_y can be designed to be robust to some modest fault conditions as well as to model uncertainties while the rest of the controllers need not consider the system faults. Therefore, the general IMC control structure alleviates the need for redesigning Q_r , Q_{l_m} , and Q_{d_m} when faults occur in the closed-loop system. What distinguishes the proposed control structure from that presented in (Zhou and Ren, 2001) is its ability to realize optimal failure-tolerant control in the case of multiple objectives.

Remark 3. Theorem 2 indicates that robust stability can be guaranteed through only the design of Q_y . However, it does not discuss robust performance, which can generally be a function of each element of Q . It is important to note that, since the control objectives can be defined with respect to any norm, we can straightforwardly build robustness into the design of Q by choosing, e.g., a weighted H_2 or H_∞ -norm. Although these choices will influence robust performance, the optimality of Q will not directly translate to optimal robust performance of the overall closed-loop system (e.g., see Zhou and Ren, 2001; Vilanova, 2007).

4. Multi-loop control systems with multiple control objectives

In this section, the proposed IMC control structure with multiple control objectives is extended for multi-loop control systems, namely cascade and coordinated control systems.

4.1. Cascade control

Cascade control systems are commonly used in the chemical industry to improve the dynamic response of the closed-loop system by effectively reducing the impact of process disturbances, in particular load disturbances (Luyben, 1973; Krishnaswamy et al., 1990). In cascade control, a secondary control loop is used to tightly control a secondary process variable that is closely related to unmeasured process disturbances, while slower measurements

of the primary process variable serve as the setpoint of the secondary control loop. The majority of cascade control systems have the series structure, where the manipulated variable influences the primary output through the secondary output (see Fig. 3a). In general, cascade control is most effective when the dynamics of the primary process exhibit nonminimum phase behavior (right-half plane zeros or a time delay) and the secondary loop has a faster dynamic response (Morari and Zafriou, 1989).

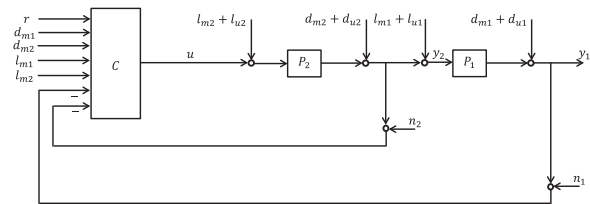
The general MC control structure for cascade control of a LTI system is obtained by replacing the plant P in the control structure of Fig. 2 with

$$\begin{bmatrix} P_1 P_2 \\ P_2 \end{bmatrix}.$$

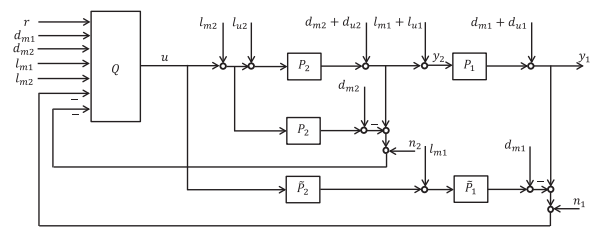
This leads to the control structure depicted in Fig. 3b with 7 degrees of freedom. The closed-loop mapping between the exogenous inputs and the two process outputs and the manipulated variable is defined by

$$\begin{bmatrix} y_1 \\ y_2 \\ u \end{bmatrix} = \mathbf{H}(P, Q_i) \begin{bmatrix} r \\ l_{m1} \\ l_{m2} \\ l_{u1} \\ l_{u2} \\ d_{m1} \\ d_{m2} \\ d_{u1} \\ d_{u2} \\ n_1 \\ n_2 \end{bmatrix},$$

where the transfer matrix $\mathbf{H}(P, Q_i)$ is



(a) Classical control structure



(b) General IMC control structure

Fig. 3. Cascade control system, where $C = [C_r C_{d_{m1}} C_{d_{m2}} C_{l_{m1}} C_{l_{m2}} C_{y1} C_{y2}]$ and $Q = [Q_r C_{d_{m1}} Q_{d_{m2}} Q_{l_{m1}} Q_{l_{m2}} Q_{y1} Q_{y2}]$.

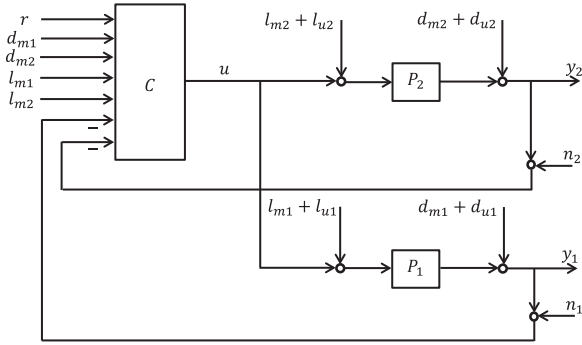


Fig. 4. Classical parallel cascade control structure, where $C = [C_r C_{d_{m1}} C_{d_{m2}} C_{l_{m1}} C_{l_{m2}} C_{y1} C_{y2}]$.

$$\begin{bmatrix} P_1 P_2 Q_r & P_1 + P_1 P_2 Q_{l_{m1}} & P_1 P_2 (I + Q_{l_{m2}}) & (I - P_1 P_2 Q_{y1}) P_1 & P_1 (I - P_2 Q_{y2}) P_2 & I + P_1 P_2 Q_{d_{m1}} \\ P_2 Q_r & I + P_2 Q_{l_{m1}} & P_2 (I + Q_{l_{m2}}) & I - P_2 Q_{y1} P_1 & (I - P_2 Q_{y2}) P_2 & P_2 Q_{d_{m1}} \\ Q_r & Q_{l_{m1}} & Q_{l_{m2}} & -Q_{y1} P_1 & -Q_{y2} P_2 & Q_{d_{m1}} \\ P_1 + P_1 P_2 Q_{d_{m2}} & I - P_1 P_2 Q_{y1} & P_1 (I - P_2 Q_{y2}) & -P_1 P_2 Q_{y1} & -P_1 P_2 Q_{y2} & \\ I + P_2 Q_{d_{m2}} & -P_2 Q_{y1} & I - P_2 Q_{y2} & -P_2 Q_{y1} & -P_2 Q_{y2} & \\ Q_{d_{m2}} & -Q_{y1} & -Q_{y2} & -Q_{y1} & -Q_{y2} & \end{bmatrix} \quad (7)$$

In the transfer matrix (7), each column depends on only one controller transfer function, so that the optimal designs of Q_i can be performed independently. The presented general cascade control structure in Fig. 3b extends the IMC cascade structure by including the effects of load disturbances and measured output disturbances on both control loops.

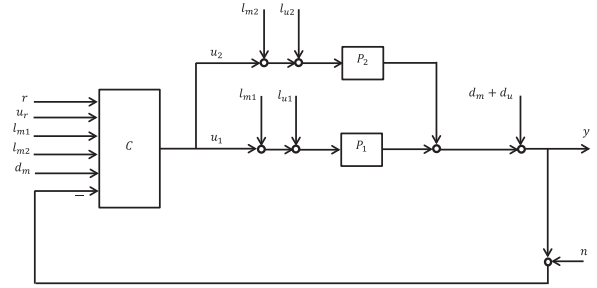
Another widely used variant of cascade control is the parallel cascade structure in which the manipulated variable affects the primary and secondary outputs through parallel actions, as shown in Fig. 4 (Luyben, 1973; Yu, 1988). Using block diagram transformations, it has been demonstrated that the parallel cascade structure is equivalent to the series cascade structure when the primary process transfer function (i.e., P_1 in Fig. 3a) is replaced with P_1/P_2 (Semino and Brambilla, 1996). Hence, the parallel cascade control structure can be derived by defining the plant as $\begin{bmatrix} P_1 \\ P_2 \end{bmatrix}$ in Fig. 2. This implies that in the cascade control structure depicted in Fig. 3b, as well as in the closed-loop mapping (7), the plant P_1 should be replaced with P_1/P_2 for the case of parallel cascade control. Note that the general IMC control structure for parallel cascade control holds only when P_2 is minimum phase.

4.2. Coordinated control

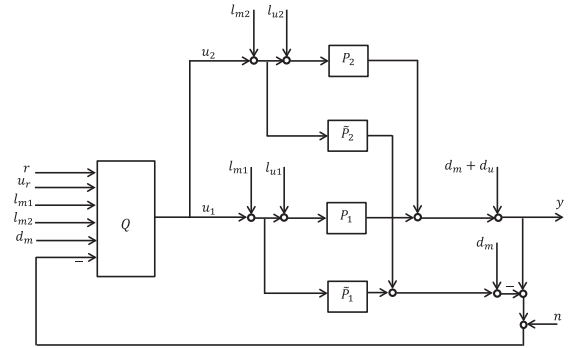
Coordinated control commonly refers to a class of control problems where two manipulated variables are used to control one output (Popiel et al., 1986; Henson et al., 1995; Giovanini, 2007; Gayadeen and Heath, 2009). A widely-used representation of coordinated control systems, also known as mid-ranging control, is depicted in Fig. 5a. A coordinated control system is designed such that the manipulated variable u_1 , which has a more direct effect on y (faster dynamics and a smaller time delay), rapidly regulates the process output for setpoint and disturbance changes. However, since the manipulation of u_1 is more expensive than u_2 , the control system gradually resets the fast input u_1 to its desired setpoint u_r as the slower input u_2 begins to affect the output.

To obtain the general structure for coordinated control of LTI systems, the plant P in the proposed control structure in Fig. 2 is replaced with

$$\begin{bmatrix} P_1 & P_2 \end{bmatrix}.$$



(a) Classical control structure



(b) General IMC control structure

Fig. 5. Coordinated control system, where $C = [C_r C_{u_r} C_{l_{m1}} C_{l_{m2}} C_{d_m} C_y]$ and $Q = [Q_r Q_{u_r} Q_{l_{m1}} Q_{l_{m2}} Q_{d_m} Q_y]$.

The resulting control structure with 6 degrees of freedom, shown in Fig. 5b, has the closed-loop mapping

$$\begin{bmatrix} y \\ u_1 \\ u_2 \end{bmatrix} = \mathbf{H}(P, Q_i) \begin{bmatrix} r \\ u_r \\ l_{m1} \\ l_{m2} \\ l_{u1} \\ l_{u2} \\ d_m \\ d_u \\ n \end{bmatrix},$$

where $H(P, Q_i)$ is defined by

$$\begin{bmatrix} (P_1 + P_2)Q_r & (P_1 + P_2)Q_{u_r} & P_1 + (P_1 + P_2)Q_{l_{m1}} & P_2 + (P_1 + P_2)Q_{l_{m2}} & (I - (P_1 + P_2)Q_y)P_1 \\ Q_r & Q_{u_r1} & Q_{l_{m1}} & Q_{l_{m2}} & -Q_y P_1 \\ Q_r & Q_{u_r2} & Q_{l_{m1}} & Q_{l_{m2}} & -Q_y P_1 \\ (I - (P_1 + P_2)Q_y)P_2 & I + (P_1 + P_2)Q_{d_m} & I - (P_1 + P_2)Q_y & -(P_1 + P_2)Q_y \\ -Q_y P_2 & Q_{d_m} & -Q_y & -Q_y \\ -Q_y P_2 & Q_{d_m} & -Q_y & -Q_y \end{bmatrix} \quad (8)$$

The closed-loop transfer matrix (8) suggests that the controllers $Q = [Q_r Q_{u_r} Q_{l_{m1}} Q_{l_{m2}} Q_{d_m} Q_y]$ are independent from each other in the general IMC coordinated control system. Note that

$$Q_{u_r} = \begin{bmatrix} Q_{u_r1} \\ Q_{u_r2} \end{bmatrix},$$

where Q_{u_r1} and Q_{u_r2} can be designed independently.

5. Design of an IMC control system with multiple objectives for a thin-film dryer

The proposed IMC control structure with multiple control objectives is demonstrated for control of a continuous dryer used for manufacturing of pharmaceutical thin-film tablets (Mesbah et al., 2014). In this process, the drug formulation solution is cast as thin films that are dried to remove solvents (volatile components) of the solution through evaporation. Among the critical quality attributes of thin films are the solvent concentration remaining in the film and the film temperature, which heavily affect the mechanical characteristics and adhesion properties of the dried films. Hence, controlling the solvent concentration and temperature of the dried films is crucial to the overall process of thin-film tablet formation.

In the thin-film dryer investigated here, the manipulated variables are flow rate of the formulation solution pumped into the dryer (u_1) and temperature of hot air exposed to the film (u_2). The measured outputs consist of solvent concentration in the film (y_1) and film temperature (y_2). The “true” dynamics of the multi-input multi-output (MIMO) thin-film drying process are described by the

first-order-plus-dead-time (FOPDT) models

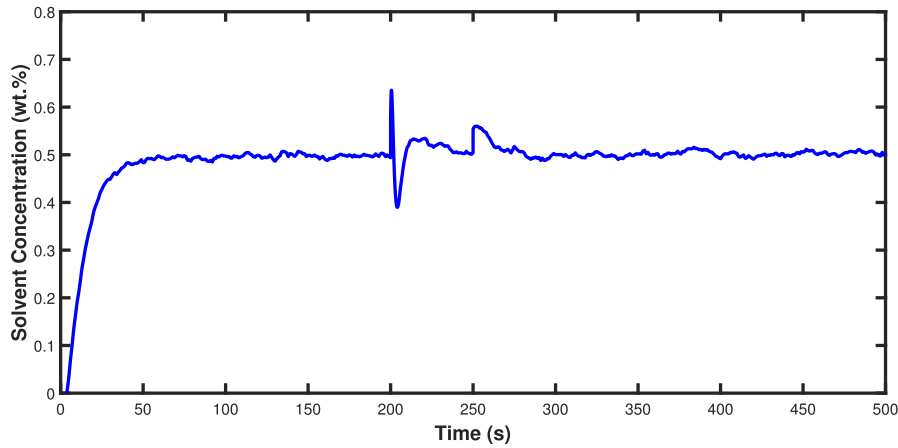
$$\begin{bmatrix} y_1 \\ y_2 \end{bmatrix} = \begin{bmatrix} p_{11} & p_{12} \\ p_{21} & p_{22} \end{bmatrix} = \begin{bmatrix} \frac{0.001e^{-5s}}{6s+1} & \frac{-0.005e^{-5s}}{3s+1} \\ \frac{-0.0003e^{-5s}}{50s+1} & \frac{0.8}{2s+1} \end{bmatrix} \begin{bmatrix} u_1 \\ u_2 \end{bmatrix}. \quad (9)$$

In this section, we apply the proposed IMC control structure to design MIMO, as well as multi-loop cascade and coordinate control systems, for regulating the solvent concentration of the dried thin films, which is considered as the primary controlled variable.

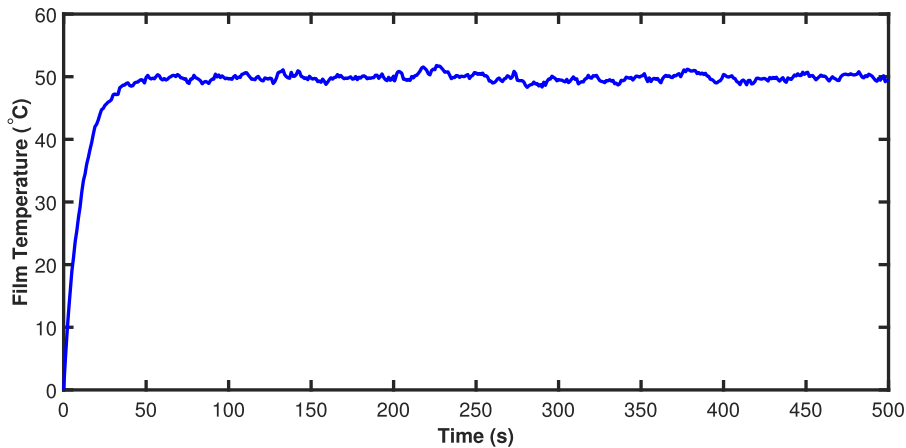
5.1. Multi-input multi-output control

A MIMO control system with multiple objectives is designed to regulate the solvent concentration in the film and the film temperature by manipulating, respectively, the feed solution pumped into the dryer and the temperature of hot air blown into the dryer. The choice of input-output pairing is informed by a singular value decomposition analysis. Measured and unmeasured disturbances are acting on the solvent concentration control loop such that

$$y_1(s) = p_{11}(s)(u_1(s) + p_{1m}(s)l_m(s)) + p_{12}(s)u_2(s) + p_{d_m}(s)d_m(s) + d_u(s),$$



(a) Solvent concentration in the film, y_1



(b) Thin-film temperature, y_2

Fig. 6. Closed-loop simulation of the MIMO control system for a step change in the reference r of the solvent concentration and film temperature feedback controllers applied at $t = 0$. The solvent concentration is affected by measured load disturbance l_m , measured output disturbance d_m , and unmeasured output disturbance d_u at $t = 150$, 200, and 250 s, respectively.

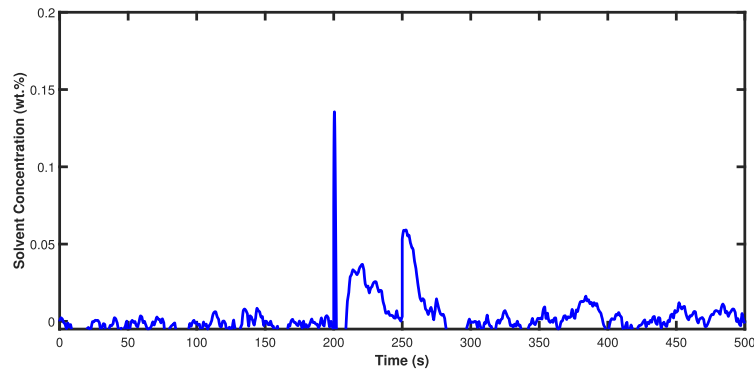
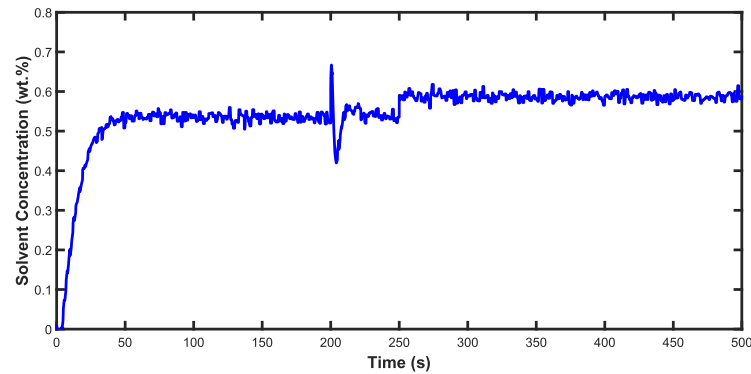
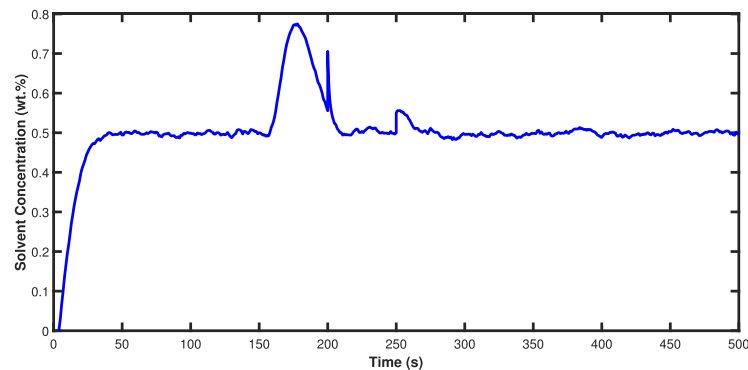
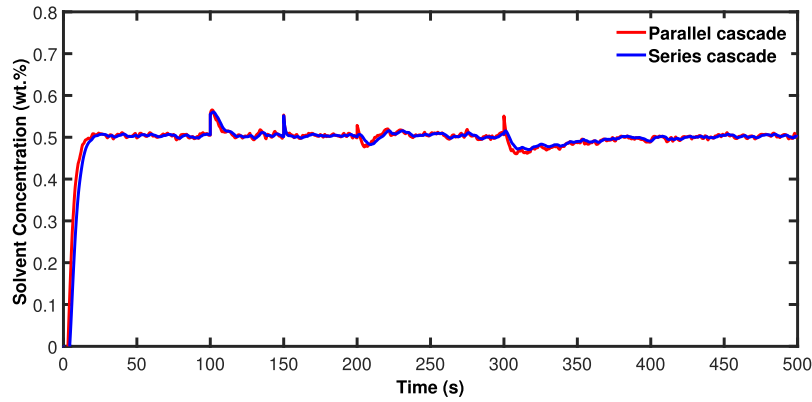
(a) Loss of the reference signal r ; Q_r is taken out of service(b) Sensor failure for y ; Q_y is taken out of service(c) Sensor failures for l_m and d_m ; Q_{l_m} and Q_{d_m} are taken out of service

Fig. 7. Closed-loop simulation of the MIMO control system during various failures in the sensors of the measurable variables for a step change in the reference r , the measured load disturbance l_m , the measured output disturbance d_m , and the unmeasured output disturbance d_u at $t = 0, 150, 200,$ and 250 s, respectively.

where $p_{l_m} = \frac{5s+10}{50s^2+10s+1}$ and $p_{d_m} = \frac{s+0.01}{s+1}$ are the measured load and output disturbance transfer functions, respectively. Solvent concentration and film temperature measurements are corrupted by sensor noise having a zero-mean Gaussian distribution with $\sigma_{y_1}^2 = 10^{-3}$ and $\sigma_{y_2}^2 = 1$, respectively.

The control objective is to track a desired setpoint for solvent concentration and film temperature, while the solvent concentration is perturbed by measured load disturbance l_m , measured output disturbance d_m , and unmeasured output disturbance d_u . The IMC control structure was used to cast the MIMO control problem

as a control design problem with multiple objectives. Four independent control objectives were formulated for solvent concentration control to realize adequate reference tracking in the presence of measured and unmeasured disturbances. H_2 -optimal IMC controllers Q_r , Q_{l_m} , Q_{d_m} , and Q_y were designed for a step change in r , l_m , d_m , and d_u , respectively, according to Theorems 3 to 6 in Appendix. The design of the IMC controllers was based on uncertain process models with 10% uncertainty in the process gains and time constants relative to the "true" process dynamics given in (9). The IMC controllers were made proper so as to be physically realizable



(a) Nominal performance

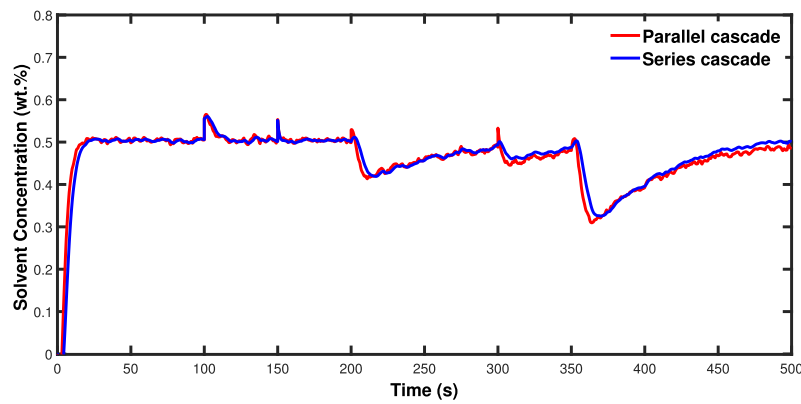
(b) Sensor failures for l_{m2} and y_2 ; $Q_{l_{m2}}$ and Q_{y2} are taken out of service

Fig. 8. Closed-loop simulation of the series and parallel cascade control systems for a step change in the reference r , the unmeasured output disturbance in the primary loop d_{u1} , the measured output disturbance in the primary loop d_{m1} , the unmeasured output disturbance in the secondary loop d_{u2} , the measured load disturbance in the primary loop l_{m1} , and the measured load disturbance in the secondary loop l_{m2} at $t = 0, 100, 150, 200, 300,$ and 350 s, respectively.

by augmenting with a first-order low-pass filter (see (13) in Appendix, where $\lambda_f = 2.0$). The time-delay terms were approximated by a first-order Padé approximation (Ogunnaik and Ray, 1994).

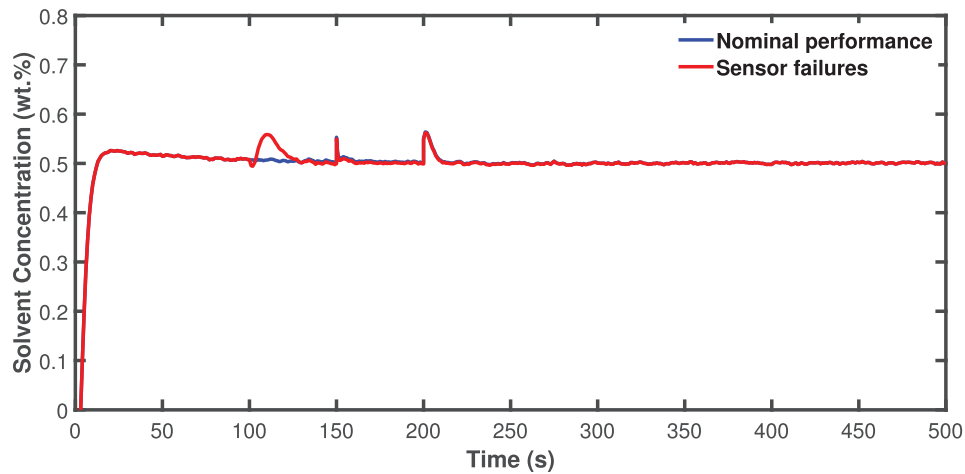
Fig. 6a shows the closed-loop profile of the solvent concentration in the thin film at the exit of the dryer when a step change is applied to the inputs r , l_m , d_m , and d_u . The response of the film temperature to a step setpoint change at time $t = 0$ is shown in Fig. 6b. The solvent concentration should be maintained at 0.5 wt.% to achieve the desired extent of drying. Fig. 6a indicates that Q_r enables very good reference tracking and the controllers Q_{l_m} , Q_{d_m} , and Q_y adequately reject the measured and unmeasured disturbances. The suppression of the measured load disturbance l_m is perfect. The closed-loop response for the measured and unmeasured output disturbances is limited by the same nonminimum phase behavior of the process. The closed-loop speed of response for the measured output disturbance and reference tracking is the same, as the two inputs act through the same controller transfer function Q_y . Additionally, Q_y handles the closed-loop interactions induced by the film temperature controller.

Next, the performance of the MIMO control system is investigated in response to failures in the sensors of the measurable variables. It is assumed that the sensor failures can be detected using fault detection and diagnosis methods (e.g., as described in Chiang et al., 2001; Gertler, 1998 and references therein). When a sen-

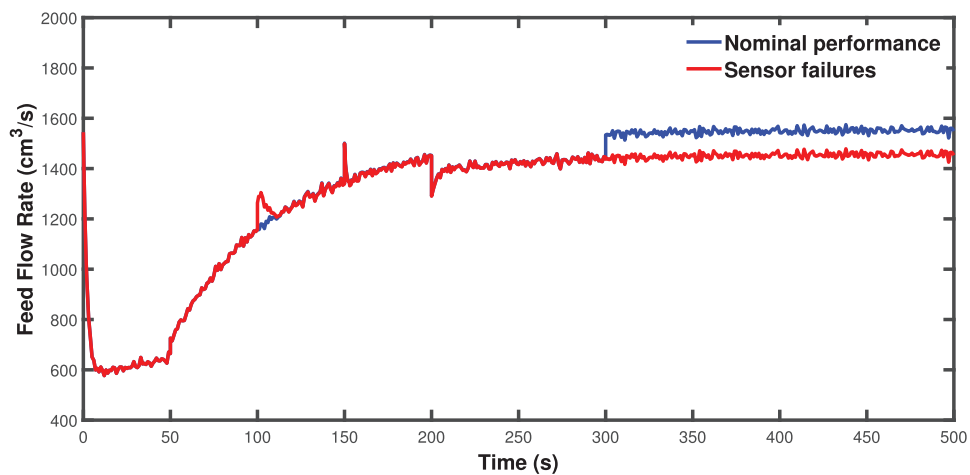
sor fails, its measurements can no longer be used for control and, therefore, the respective controller is switched off. Fig. 7 shows the system response in the event of sensor failures for the measurable variables r , l_m , d_m , and y . The solvent concentration profiles indicate that the closed-loop system response to the measurable variables with working sensors remains unaffected by removal of the failed sensors, as suggested by the analysis in Section 3.

Fig. 7a shows the solvent concentration response for a loss in the reference signal, which could occur due to loss in a communication line between an upper-level supervisory control loop and a lower-level regulatory control system. The comparison between Figs. 6 and 7a reveals that the solvent concentration response to the disturbances l_m , d_m , and d_u is completely unaffected by the loss of reference signal, as the response is just shifted to a different baseline. Fig. 7b suggests that the closed-loop response to the exogenous inputs r , l_m , and d_m is completely unaffected by a failure in the output sensor y . This results from the fact that the feedforward controllers Q_r , Q_{l_m} , and Q_{d_m} remain intact by the loss in the feedback of y . Under these conditions, only the output response to the unmeasured disturbance is influenced by the loss of y , as the measurement of the output is the only way by which the control system can detect the presence of d_u .

Fig. 7c indicates that losing the controller Q_{l_m} affects the closed-loop response at $t = 150$ s while having no effect on the closed-



(a) Process output (solvent concentration)



(b) Fast manipulated variable (feed flow rate)

Fig. 9. Closed-loop simulation of the coordinated control system for a step change in the reference r , the measured load disturbance for the slow input l_{m2} , the measured load disturbance for the fast input l_{m1} , the measured output disturbance d_m , the unmeasured output disturbance d_u , and the input setpoint u_r at $t = 0, 50, 100, 150, 200,$ and 300 s, respectively.

loop response to the reference signal r and unmeasured output disturbance d_u . The integrating action of Q_y forces the output response to follow the reference signal r after the measured load disturbance perturbs the system. Fig. 7c also suggests that the loss of the measured output disturbance signal d_m and, consequently, the controller Q_{d_m} does not influence the output responses of the working sensors Q_x and Q_y . This numerical example clearly demonstrates the optimal failure tolerance of the proposed IMC control structure and controller design method. It illustrates that the control structure alleviates the need to redesign controllers for optimal failure-tolerant control.

5.2. Cascade control

We now use the hot air temperature (i.e., manipulated variable) to control the solvent concentration in the thin-film (i.e., primary process output), while the thin-film temperature is used as the secondary process output. Leveraging the single manipulated variable and the two measured outputs, the goal is to design a cascade control system with multiple objectives. The process dynam-

ics (9) implies that manipulation of the hot air temperature has a much faster influence on the film temperature dynamics (p_{22}) than on the solvent concentration dynamics (p_{21}). This suggests that the film temperature, which is closely related to the solvent concentration in the film (the primary process output) and is readily available from on-line measurements, can be used to improve the dynamic response of the closed-loop system in terms of disturbance rejection. The process is under the influence of various disturbances such that the secondary process output (film temperature, y_2) and the primary process output (solvent concentration, y_1) are described by

$$y_2(s) = p_{22}(s)(u(s) + l_{m2}(s)) + d_{u2}(s)$$

and

$$y_1(s) = p_{21}(s)(y_2(s) + l_{m1}(s)) + p_{d_{m1}}(s)d_{m1}(s) + d_{u1}(s),$$

respectively, where u is the hot air temperature and $p_{d_{m1}} = \frac{s+0.01}{s+1}$ (see Fig. 3b for the cascade IMC control structure). Both process outputs are corrupted by stochastic sensor noise defined as in Section 5.1.

The control objective is to maintain the solvent concentration at a predetermined setpoint r in the presence of the different measured and unmeasured disturbances (l_{m1} , l_{m2} , d_{u1} , d_{u2} , and d_{m1}) acting on the process. The cascade IMC control structure presented in Section 4.1 was applied to formulate the control design problem with multiple objectives for the series and parallel cascade control systems. H_2 -optimal IMC controllers were designed using the results of Theorems 3 to 6 in Appendix for a step change in the input and, subsequently, augmented with a first-order low-pass filter (see (13) in Appendix, where $\lambda_f = 2.0$).

Fig. 8a shows the closed-loop response of the primary process output for both cascade control systems. The optimal design of Q_r results in perfect reference tracking, while the feedforward controllers $Q_{l_{m1}}$, $Q_{l_{m2}}$, and $Q_{d_{m1}}$ along with the feedback controllers Q_{y1} and Q_{y2} adequately reject all the disturbances affecting the system. For the thin-film drying process investigated here, Fig. 8a indicates that the series and parallel cascade control systems exhibit comparable performance under the nominal process operation. Note that the proposed control structure provides a consistent framework to evaluate the performance of the cascade control systems since the performance comparison is independent of the choice of the controller tuning.

Fig. 8b depicts the closed-loop system response for the two cascade control systems when the sensors used to measure the secondary load disturbance (l_{m2}) and the secondary process output (y_2) failed. Failure of the latter sensors rendered the secondary control loop in the cascade structures dysfunctional, as $Q_{l_{m2}}$ and Q_{y2} were switched off. Fig. 8b suggests that the series cascade control system outperforms the parallel cascade system in the event of sensor failures. This is because of the longer response time of the parallel control system to restore the performance (bring the solvent concentration to its setpoint) once the load disturbance l_{m2} occurred at 350 s. Yet, the performance of the rest of the optimal controllers in both control systems remains intact due to optimal failure tolerance of the control structure.

5.3. Coordinated control

We now aim to control the solvent concentration in the thin film by manipulating the hot air temperature and feed flow rate in a coordinated manner. The process dynamics (9) suggest that manipulation of the feed flow rate for controlling the solvent concentration (p_{11}) exhibits much faster dynamics than using the hot air temperature (p_{21}). Hence, manipulating the feed flow rate enables obtaining a better closed-loop response in terms of setpoint tracking and disturbance rejection. However, the feed flow rate should be reset to a predetermined setpoint during process operation to achieve a desired production rate.

Consider the process to be affected by various disturbances such that solvent concentration is described by

$$y(s) = p_1(s)(u_1(s) + l_{m1}(s)) + p_2(s)(u_2(s) + l_{m2}(s)) + p_{d_m}(s)d_m(s) + d_u(s),$$

where $u_1(s)$ and $u_2(s)$ are the fast manipulated variable (feed flow rate) and slow manipulated variable (hot air temperature), respectively. The coordinated control system is depicted in Fig. 5b. The control objective is not only to regulate the solvent concentration in the presence of disturbances (l_{m1} , l_{m2} , d_m , and d_u), but also to reset the feed flow rate to its desired setpoint u_r as the slow manipulated variable begins to influence the output. The analytical expressions for H_2 -optimal IMC controllers were derived for a step input. The tuning parameter of the first-order low-pass filter (13) was set to $\lambda_f = 2.0$.

Fig. 9 shows the closed-loop response of the system under the nominal process operation and the case of system failures due to

loss of the measured load disturbance signal l_{m1} and the input setpoint signal u_r . Fig. 9a suggests that the loss of l_{m1} at 100 s is merely detrimental to the ability of the control system in rejecting the load disturbance affecting the fast control loop, as the rest of the controllers fulfill their objectives adequately. It is shown in Fig. 9b that losing the input setpoint at 300 s (e.g., due to a communication failure between supervisory and regulatory control levels) only makes the control system unable to maintain the feed flow rate at its desired level $1550 \text{ cm}^3/\text{s}$. The simulation results indicate that, in the event of sensor failures, the optimal performance of the coordinated control system is preserved with respect to the working controllers.

6. Conclusions

We presented a general control structure for designing control systems with multiple objectives related to reference tracking and rejection of load and output disturbances for LTI systems. The proposed control structure is an extension of the internal model control structure to systems with four degrees-of-freedom. Through Youla parameterization of all stabilizing controllers, it is demonstrated that the control structure is non-restrictive in terms of the achievable performance. The distinct feature of the control structure is that the controllers can be designed independently from each other, as the control objectives are defined separately for each exogenous input. This feature is particularly significant for failure-tolerant control since the optimal performance of the remaining controllers will remain intact when any controller is taken off due to actuator and/or sensor failures. We note that the proposed control structure can in principle complement model predictive control (MPC) when used as a failure-tolerant regulatory control system. Although MPC is especially well suited for optimal control of constrained multivariable systems, failure tolerance in MPC is particularly challenging and largely remains an open area of research (e.g., see Zhang and Jiang, 2008). This challenge mainly arises from the fact that MPC inherently accounts for multivariable system interactions, which is in contrast to the proposed control structure that decouples the multiple control objectives in order to individually leverage the degrees of freedom in the process. Thus, the integration of the proposed control structure and MPC is an interesting potential direction for future research.

Declaration of Competing Interest

We declare no conflict of interest.

Acknowledgments

The authors wish to thank Novartis Pharma AG for financial support.

Appendix A

Consider a LTI single-input single-output process $p(s)$

$$p(s) = p_a(s)p_m(s), \quad (10)$$

where $p_a(s)$ and $p_m(s)$ are the all-pass and minimum-phase parts of $p(s)$, respectively. $p_a(s)$ includes the right-half plane zeros, as well as time delays of $p(s)$, and generally takes the form

$$p_a(s) = e^{-\theta s} \prod_i \frac{-s + \zeta_i}{s + \zeta_i^*},$$

where the superscript $*$ denotes complex conjugate (Morari and Zafriou, 1989). Below, optimal control designs are obtained for the controllers in the control structure in Fig. 2 for the single-input single-output process (10). The control objectives are defined

in terms of minimization of the H_2 -norm of the columns of the closed-loop transfer function $\mathbf{H}(P, Q_i)$ (see (5)). As derivation of analytical expressions for controllers requires partial fraction expansion, the main result of partial fraction expansion is summarized in Definition 3.

Definition 3. (Partial fraction expansion (Polderman and Willems, 1998)): Suppose $A(s) = \prod_{i=1}^N (s - \lambda_i)^{n_i}$, $\lambda_i \neq \lambda_j$, $i \neq j$, with integers n_i and $\deg B(s) \leq \deg A(s)$. The partial fraction expansion of $A^{-1}(s)B(s)$ is defined by

$$A^{-1}(s)B(s) = a_0 + \sum_{i=1}^N \sum_{j=1}^{n_i} \frac{a_{ij}}{(s - \lambda_i)^j}, \quad (11)$$

where

$$B(s) = a_0 A(s) + \sum_{i=1}^N \sum_{j=1}^{n_i} a_{ij} \left(\prod_{k \neq i} (s - \lambda_k)^{n_k} \right) (s - \lambda_i)^{n_i - j} \quad (12)$$

$$a_0 = \lim_{s \rightarrow \infty} \frac{B(s)}{A(s)}$$

$$a_{in_i} = \lim_{s \rightarrow \lambda_i} (s - \lambda_i)^{n_i} \frac{B(s)}{A(s)} \quad i = 1, \dots, N,$$

$$a_{ij} = \lim_{s \rightarrow \lambda_i} (s - \lambda_i)^j \left(\frac{B(s)}{A(s)} - \sum_{k=j+1}^{n_i} \frac{a_{ik}}{(s - \lambda_i)^k} \right) \quad i = 1, \dots, N,$$

$$j = 1, \dots, n_i - 1.$$

The following theorems give analytical expressions for H_2 -optimal controllers Q_r , Q_{I_m} , Q_{d_m} , and Q_y . The proof of the theorems below follows from Theorem 4.1-1 in (Morari and Zafriou, 1989).

Theorem 3. Consider the stable process $p(s)$ defined as in (10). Let a proper weight function $r(s)$ be factored into an all-pass part and a minimum-phase part

$$r(s) = r_a(s)r_m(s) = r_a(s) \frac{r_n(s)}{r_d(s)}.$$

Then the optimal solution to $\inf_{Q_r} \|(pQ_r - 1)r\|_2$ is

$$Q_r = \frac{B(s)}{p_m(s)r_n(s)},$$

where $B(s)$ is calculated from (12) for

$$\frac{A(s)}{B(s)} = \frac{r_n(s)}{p_a(s)r_d(s)}$$

with λ_i being the zeros of $r_d(s)$.

Theorem 4. Consider the stable process $p(s)$ defined as in (10). Then the optimal solution to $\inf_{Q_{I_m}} \|p(1 + Q_{I_m})I\|_2$ is

$$Q_{I_m} = -1.$$

Theorem 5. Consider the stable process $p(s)$ defined as in (10). Let the minimum-phase part of a proper weight function $d(s)$ be written as $d_n(s)/d_d(s)$. Then the optimal solution to $\inf_{Q_{d_m}} \|(1 + pQ_{d_m})d\|_2$ is

$$Q_{d_m} = \frac{-B(s)}{p_m(s)d_n(s)},$$

where $B(s)$ is calculated from (12) for

$$\frac{A(s)}{B(s)} = \frac{d_n(s)}{p_a(s)d_d(s)}$$

with λ_i being the zeros of $d_d(s)$.

Theorem 6. Consider the stable process $p(s)$ defined as in (10). Let the minimum-phase part of a proper weight function $v(s) = p(s)l_u(s) + d_u(s)$ be written as $v_n(s)/v_d(s)$. Then the optimal solution to $\inf_{Q_y} \|(1 - pQ_y)v\|_2$ is

$$Q_y = \frac{B(s)}{p_m(s)v_n(s)},$$

where $B(s)$ is calculated from (12) for

$$\frac{A(s)}{B(s)} = \frac{v_n(s)}{p_a(s)v_d(s)}$$

with λ_i being the zeros of $v_d(s)$.

The above analytical expressions obtained for the optimal controllers are stable but may be improper and, as a result, the controllers may be physically unrealizable. In the IMC control design method (Morari and Zafriou, 1989), the optimal controllers are augmented with a low-pass filter such as

$$J_f(s) = \frac{1}{(\lambda_f s + 1)^{n_f}}, \quad (13)$$

with n_f just large enough that the controllers Q_i are proper, at the expense of sub-optimality.² In (13), λ_f is an adjustable parameter, with small values leading to very fast response and large values resulting in manipulated variable moves that are slower and have smaller peak values during sharp changes in the inputs.

References

Blanke, M., Kinnaert, M., Lunze, J., Staroswiecki, M., 2003. Diagnosis and Fault-Tolerant Control. Springer-Verlag, New York.

Braatz, R.D., 1996. Internal Model Control. CRC Press, Florida, pp. 215–224.

Brosilow, C., Markale, N., 1992. Model predictive cascade control and its implications for classical and IMC cascade control. Miami

Chiang, L.H., Russell, E.L., Braatz, R.D., 2001. Fault Detection and Diagnosis in Industrial Systems. Springer-Verlag, London.

Curtain, R.F., Zwart, H., 1995. An Introduction to Infinite-Dimensional Linear Systems Theory. Springer-Verlag, New York.

Dehghani, A., Lanzon, A., Anderson, B.D.O., 2006. A two-degree-of-freedom H_∞ control design method for robust model matching. Int. J. Robust Nonlinear Control 16, 467–483.

Gayadeen, S., Heath, W., 2009. An internal model control approach to mid-ranging control, pp. 542–547.

Gertler, J.J., 1998. Fault Detection and Diagnosis in Engineering Systems. Marcel Dekker, New York.

Giovanini, L., 2007. Cooperative-feedback control. ISA Trans. 46, 289–302.

Grimble, M.J., 1988. Two-degrees of freedom feedback and feedforward optimal control of multivariable stochastic systems. Automatica 24, 809–817.

Henson, M.A., Ogunnaike, B.A., Schwaber, J.S., 1995. Habituating control strategies for process control. AIChE J. 41, 604–617.

Horn, I.G., Arulandu, J.R., Gombas, C.J., VanAntwerp, J.G., Braatz, R.D., 1996. Improved filter design in internal model control. Ind. Eng. Chem. Res. 35, 3437–3441.

Isermann, R., 2006. Fault Diagnosis Systems: An Introduction from Detection to Fault Tolerance. Springer-Verlag, Berlin.

Krishnaswamy, P.R., Rangaiah, G.P., Jha, R.K., Deshpande, P.B., 1990. When to use cascade control? Ind. Eng. Chem. Res. 29, 2163–2166.

Limebeer, D.J.N., Kasenally, E.M., Perkins, J.D., 1993. On the design of robust two degree of freedom controllers. Automatica 29, 157–168.

Liu, T., Zhang, W., Gao, F., 2007. Analytical two-degrees-of-freedom (2-DOF) decoupling control scheme for multi-input multi-output (MIMO) processes with time delays. Ind. Eng. Chem. Res. 46, 6546–6557.

Luyben, W.L., 1973. Parallel cascade control. Ind. Eng. Chem. Fundam. 12, 463–467.

Mesbah, A., Braatz, R.D., 2013. Design of multi-objective control systems with optimal failure tolerance, pp. 2963–2968. Zurich

Mesbah, A., Kishida, M., Braatz, R.D., 2013. Design of multi-objective failure-tolerant control systems for infinite-dimensional systems, pp. 3006–3013. Florence

Mesbah, A., Versypt, A.N.F., Zhu, X., Braatz, R.D., 2014. Nonlinear model-based control of thin-film drying for continuous pharmaceutical manufacturing. Ind. Eng. Chem. Res. 53, 7447–7460.

Morari, M., Zafriou, E., 1989. Robust Process Control. Prentice-Hall, New Jersey.

Ogunnaike, B.A., Ray, W.H., 1994. Process Dynamics, Modeling, and Control. Oxford University Press, New York.

Polderman, J.W., Willems, J.C., 1998. Introduction to Mathematical Systems Theory: A Behavioral Approach. Springer-Verlag, New York.

Popiel, L., Matsko, T., Brosilow, C., 1986. Coordinated control, pp. 295–319. New York

Pottmann, M., Henson, M.A., Ogunnaike, B.A., Schwaber, J.S., 1996. A parallel control strategy abstracted from the baroreceptor reflex. Chem. Eng. Sci. 51, 931–945.

Paulson, Joel A, Heirung, Tor Aksel N, Mesbah, Ali, 2019. Fault-Tolerant Tube-Based Robust Nonlinear Model Predictive Control. In Proceedings of the American Control Conference, 1648–1654.

Semino, D., Brambilla, A., 1996. An efficient structure for parallel cascade control. Ind. Eng. Chem. Res. 35, 1845–1852.

² Somewhat more complicated filters are more appropriate in the presence of load disturbances when the closed-loop dynamics are much faster than the open-loop process dynamics (Horn et al., 1996).

- Skogestad, S., Postlethwaite, I., 1996. *Multivariable Feedback Control: Analysis and Design*. Wiley, New York.
- Tan, W., Marquez, H.J., Chen, T., 2003. IMC Design for unstable processes with time delays. *J. Process Control* 13 (3), 203–213.
- Vidyasagar, M., 2011. *Control System Synthesis: A Factorization Approach*, vol. 2. Morgan & Claypool Publishers.
- Vilanova, R., 2007. Feedforward control for uncertain systems. internal model control approach, pp. 418–425. Patras, Greece
- Vilanova, R., Serra, I., Pedret, C., Moreno, R., 2006. Reference processing in two-degree-of-freedom control: Separation, independence or optimality, pp. 5680–5685. Minneapolis
- Yu, C.-C., 1988. Design of parallel cascade control for disturbance rejection. *AIChE J.* 34, 1833–1838.
- Zhang, Y., Jiang, J., 2008. Bibliographical review on reconfigurable fault-tolerant control systems. *Annu. Rev. Control* 32 (2), 229–252.
- Zhou, D.H., Frank, P.M., 1998. Fault diagnostics and fault tolerant control. *IEEE Trans. Aerosp. Electron. Syst.* 34, 420–427.
- Zhou, K., Doyle, J.C., Glover, K., 1996. *Robust and Optimal Control*. Prentice-Hall, New Jersey.
- Zhou, K., Ren, Z., 2001. A new controller architecture for high performance, robust, and fault-tolerant control. *IEEE Trans. Automat. Control* 46, 1613–1618.